Received: 30 April 2024 | Accepted: 11 August 2024

DOI: 10.1002/lio2.70007

ORIGINAL RESEARCH

Laryngoscope Investigative Otolaryngology

Immunocytochemistry assessment of vocal fold regeneration after cell-based implant in rabbits

Larissa Nicolas BS[1] | Hanna Mandl BS[1] | Feng Schrader BS[2] | Jennifer L. Long MD, PhD[2,3]

[1]David Geffen School of Medicine at University of California-Los Angeles, Los Angeles, California, USA

[2]Research Service, Greater Los Angeles VAHS, Los Angeles, California, USA

[3]Department of Head and Neck Surgery, David Geffen School of Medicine at University of California-Los Angeles, Los Angeles, California, USA

Correspondence
Jennifer L. Long, Department of Head and Neck Surgery, David Geffen School of Medicine at UCLA, 650 Charles Young Drive, CHS room 62-132, Los Angeles, CA 90095, USA.
Email: jlong@mednet.ucla.edu

Funding information
National Institutes of Health, Grant/Award Number: NIDCD R01 DC016959; U.S. Department of Veteran Affairs, Rehabilitation Research and Development, Grant/Award Number: I01RX003649; NIH National Center for Advancing Translational Science, Grant/Award Number: UL1TR001881; UCLA Jonsson Comprehensive Cancer Center

Abstract

Objective: Cell-based outer vocal fold replacement (COVR) offers a potential treatment for severe vocal fold scarring or cancer reconstruction. Previous work in rabbits using human adipose-derived stem cells (ASC) in fibrin suggested that a hybrid structure emerged within 2 months, containing both implanted and host cells. This project uses immunocytochemistry to better define the phenotypic fate of implanted cells and features of the extracellular environment.

Methods: Immunocytochemistry was performed on sections collected from rabbits 2 months after COVR implantation or scar surgery. Cellular targets included human leukocyte antigen (HLA), CD31, and smooth muscle actin (SMA).

Results: HLA was present in all implanted sections and was used to identify human cells. In adjacent sections, HLA-positive cells were identified expressing CD31. SMA was not identified in the same cells as HLA. These markers were also present in injured vocal folds not receiving COVR. SMA protein content did not differ according to treatment.

Conclusions: Implanted human ASC persist in rabbit vocal folds. Some appear to express CD31, an endothelial marker. Smooth muscle actin, a marker of myofibroblast phenotype, was present in all sections regardless of treatment, and was not identified in hASC. Host cells also infiltrate the structure, producing a hybrid host-graft vocal fold.

KEYWORDS
angiogenesis, cell-based implant, human adipose derived stem cells, smooth muscle actin, vocal fold regeneration

1 | INTRODUCTION

The human vocal folds (VF) are intricate structures composed of a specialized lamina propria (LP) and stratified squamous epithelium. Vocal fold scarring is a prevalent condition that can significantly impair voice quality and function.[1] This debilitating issue can arise from various etiologies, including surgical interventions, trauma, radiation therapy, and vocal misuse. The pathophysiology of VF scarring involves inflammation and fibrosis, which can lead to severe dysphonia or aphonia.[2]

Despite the availability of treatment options such as pharmacotherapy, voice therapy, and surgical interventions, these solutions have remained suboptimal in restoring the biomechanical properties of the VF LP.[3–5] Research has not definitively supported the

This work was presented at the 2024 Combined Otolaryngology Spring Meeting in Chicago, IL, May 16–18.

superiority of any particular therapeutic method,[6] underscoring the need for more effective approaches.

In this context, the use of regenerative medicine has emerged as a promising avenue for addressing vocal fold scarring. Much of the work within this area has focused on cell therapy, scaffold development, or the utilization of specific growth factors.[7] Approaches involving embryonic stem cells,[8] human mesenchymal stem cells from bone marrow[9] or adipose tissue,[10,11] and human amniotic epithelial cells[12] have demonstrated promising results.

To further advance the field, we have developed a novel cell-based outer vocal fold replacement (COVR) approach. This tissue-engineered implant consists of human adipose-derived stem cells (hASCs) within a fibrin matrix, aiming to promote the regeneration of scarred vocal folds. Results in rabbits have shown that the COVR approach facilitated the formation of a hybrid structure with sustained human leukocyte antigen (HLA) expression after two months[13,14] and donor cell DNA was detected at 4 weeks.[15]

However, the presence of HLA alone does not provide information on the integration and functionality of the implant within the host tissue. In our current research, we seek to better define the phenotypic fates of the implanted human adipose-derived stem cells (hASCs) as they relate to two domains of interest for vocal fold wound healing: fibroblast activation state and angiogenesis.

2 | MATERIALS AND METHODS

2.1 | In vitro culture and COVR fabrication

The experimental setup mirrored the established protocols that have been previously described.[16] To summarize, hASCs were sourced from the American Type Culture Collection and underwent expansion under conventional culture conditions. COVR implants were crafted through a combination of hASC, rabbit fibrinogen (obtained from innovative research), and bovine thrombin (sourced from Sigma-Aldrich) in a 4:1:1 ratio. Each 600 µl COVR gel encapsulated a total of 600,000 cells to replicate the cellular density found in VF LP. The solutions were blended within 12-mm Transwell inserts from Corning and left to incubate at 37C, with gelation occurring swiftly within 30 min. Differentiation medium enriched with 10 ng/mL human recombinant EGF from Promega Corp was administered at the basal surface. After a 2-week cultivation period, the developed COVR was harvested for transplantation by incising and peeling the Transwell membrane away from the insert and gel, although preserving the lumenal-basal orientation. The resultant COVR constructs measured 12 mm in diameter with thicknesses ranging between 2–3 mm.

2.2 | Implantation in rabbit model

All animal procedures were conducted in accordance with the Public Health Service Policy on Humane Care and Use of Laboratory Animals, the NIH Guide for the Care and Use of Laboratory Animals, and the Animal Welfare Act, and were approved by the local Institutional Animal Care and Use Committee. New Zealand white rabbits from two separate implantation series were examined here. In the first set, bilateral COVR implant was performed in 3 male and 3 female rabbits at the time of VF injury, then allowed to heal for two months. One additional male had preoperative poor feeding but proceeded with a bilateral COVR implant. Hypoxia developed during wound closure, and the animal was humanely euthanized although still in the operative suite. Necropsy and larynx harvest were completed immediately, which revealed severe pulmonary edema manifested as pink frothy fluid filling the lungs. That animal is reported as "Day 0".

A separate set of slides were obtained from animals reported in a prior study.[14] Briefly, these were randomly allocated to one of three treatment groups: (1) open transcervical unilateral cordectomy followed by immediate COVR implantation (acute COVR group); (2) endoscopic unilateral cordectomy followed by transcervical COVR implantation 2 months later (chronic COVR group); or (3) endoscopic unilateral cordectomy with transcervical sham surgery 2 months later (chronic scar group).

COVR implants were performed as previously described.[13,14] Vertical neck incision exposed the larynx and trachea, and a temporary tracheotomy provided airway control during the surgery only. Laryngofissure revealed the endolarynx. Vibratory mucosa from one or both VF was excised through sharp dissection, down to the thyroarytenoid muscle. The COVR gel was applied to the defect and secured in place with anterior and posterior sutures of 5–0 fast gut. The larynx was closed with a Prolene suture, an endotracheal tube was removed, and layered wound closure was performed. Perioperative antibiotics and corticosteroids were administered for 3 days. Following the 2-month maturation period, the animals were euthanized for larynx retrieval.

2.3 | Tissue harvest and processing

The excised larynges from the first group (with bilateral COVR) were bisected into hemilarynges. One hemilarynx was fixed in formalin, embedded within paraffin, and then sectioned for analysis. The other hemilarynx was used for molecular studies, which are ongoing. The excised larynges from the second group (with unilateral injury or implant) were initially studied with ex vivo phonation and indentation, as previously described.[14] They were then bisected into hemilarynges, immersed in OCT freezing compound, and flash frozen in liquid nitrogen for frozen section cutting. Some microscopic findings were previously reported, and additional imaging was performed here.

2.4 | Histology, immunohistochemistry, and microscopy

The formalin-fixed, paraffin-embedded (FFPE) slides were first rehydrated by immersing the samples for 5 min each under the following solutions: 100% xylene, 100% ethanol, 70% ethanol, and dH2O. One

section of each animal was used for Pentachrome histological staining to show elastic fibers in black, collagen in yellow-brown, muscle in fuschia, and glycosaminoglycans in blue. Pentachrome slides were digitally scanned to show the entire section at 4X magnification.

For FFPE slides undergoing immunocytochemistry, antigen retrieval was performed by boiling in citrate acid buffer (ph 6) and then maintained at a sub-boiling temperature for 20 min. After cooling for an additional 20 min the sections were immersed in distilled water for five minutes and then washed with PBS. Slides were blocked with 5% goat serum diluted in PBS for 30 min. Primary antibody staining was done with either anti-HLA (Abcam cat#: ab70328) at a 1:500 dilution or anti-CD31 (Novus cat#: NB0122181) at a 1:400 dilution. Primary antibody was added in 1% BSA (1:500 dilution) to slides and stored overnight for 20 h. A negative control slide receiving only 1% BSA without primary antibody was performed for each animal. Secondary antibody staining was done with 2.5% goat serum blocking solution for 15 min. Fluorescently labeled secondary antibody, goat-anti mouse (Alexa Flour 633, Thermal Fisher), in 1% BSA (1:400 dilution) was later added.

Frozen sections were prepared for immunocytochemistry in a similar fashion except without antigen retrieval. Some of these slides were also labeled with alpha-smooth muscle actin (SMA) antibodies at a dilution of 1:500. The secondary antibody was performed the same as in the paraffin slides. All sections received one drop of antifade mounting medium with DAPI (Vectashield) prior to the addition of a cover slide.

2.5 | Western blot analysis

Frozen sections from operated vocal folds were scraped off slides and collected for protein. Cells and tissue were lysed in an SDS sample solution containing 2% SDS and 10% glycerol in 0.5 M Tris-buffer at pH 7.5. The lysates were snap-frozen in liquid nitrogen to prevent degradation. Approximately 300 µL of ice-cold lysis buffer was rapidly added to 5 mg of tissue, which was then homogenized using an electric homogenizer. The lysate was centrifuged at 12,000 rpm for 20 min at 4°C, and the supernatant was collected. The lysate was then heated in a sample buffer at 100°C for 5 min. Samples were loaded onto a 10% Mini-PROTEAN TGX precast gel and resolved by SDS-PAGE at 120 V for 85 min. The resolved proteins were transferred from the gel to a PVDF membrane at 100 mA for 1.5 h. The membrane was blocked for 30 min and then incubated with the primary antibody, anti-SMA (1:2000), or B-actin as a loading control, for 1.5 h at room temperature. After washing, the membrane was incubated with the secondary antibody, Goat anti-Mouse IgG-HRP (1:3000), for 75 min. Proteins were detected using an ECL chemiluminescent system, with optimal exposure time between 30–300 s.

Quantification of Western Blot lanes was done through the utilization of ImageJ Software (https://imagej.net/ij/) and analysis was performed through the Gel Analysis methods outlined in ImageJ[17] with reference to an identical protocol as discussed by Stael.[18]

Animal #	HLA+ Cells	CD31+ Cells
M-1	Few	Some
M-2	Some	Some
M-3	Some	Few
F-1	Some	Some
F-2	Some	Some
F-3	Few	Few
M-Day 0	Many	Many non-cellular

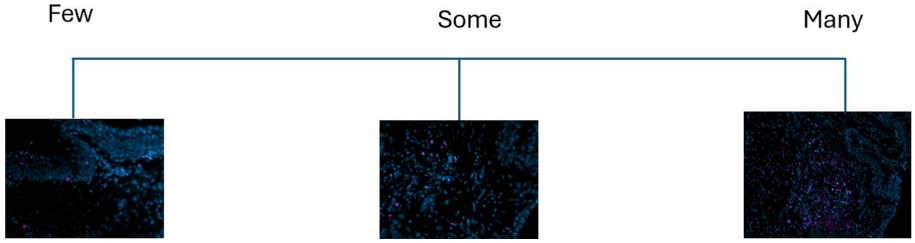

FIGURE 1 Rating of HLA and CD31+ Cells in COVR Implanted Tissue. The chart provides an overview regarding the presence of positively stained cells within paraffin-embedded tissue. All animals that were analyzed underwent COVR implantation after injury. More than three images were taken from each slide and were then visually inspected for the presence of HLA and CD31-positive cells. The diagram at the bottom of the chart provides examples of the "Few", "Some", and "Many" rating schemes.

Individual bands of the gels were marked with rectangular selections within the ImageJ Software. Intensity profile plots were then created for each band, and total intensity was calculated using the "Plot profile" function. The intensity of SMA was corrected by our loading protein, B-actin, through utilization of the formula (SMA / (SMA + B-actin)).

3 | RESULTS

3.1 | Human leukocyte antigen expression

HLA labeling was identified in scattered cells within the implant region in all animals receiving COVR (Figure 1). The frozen section findings

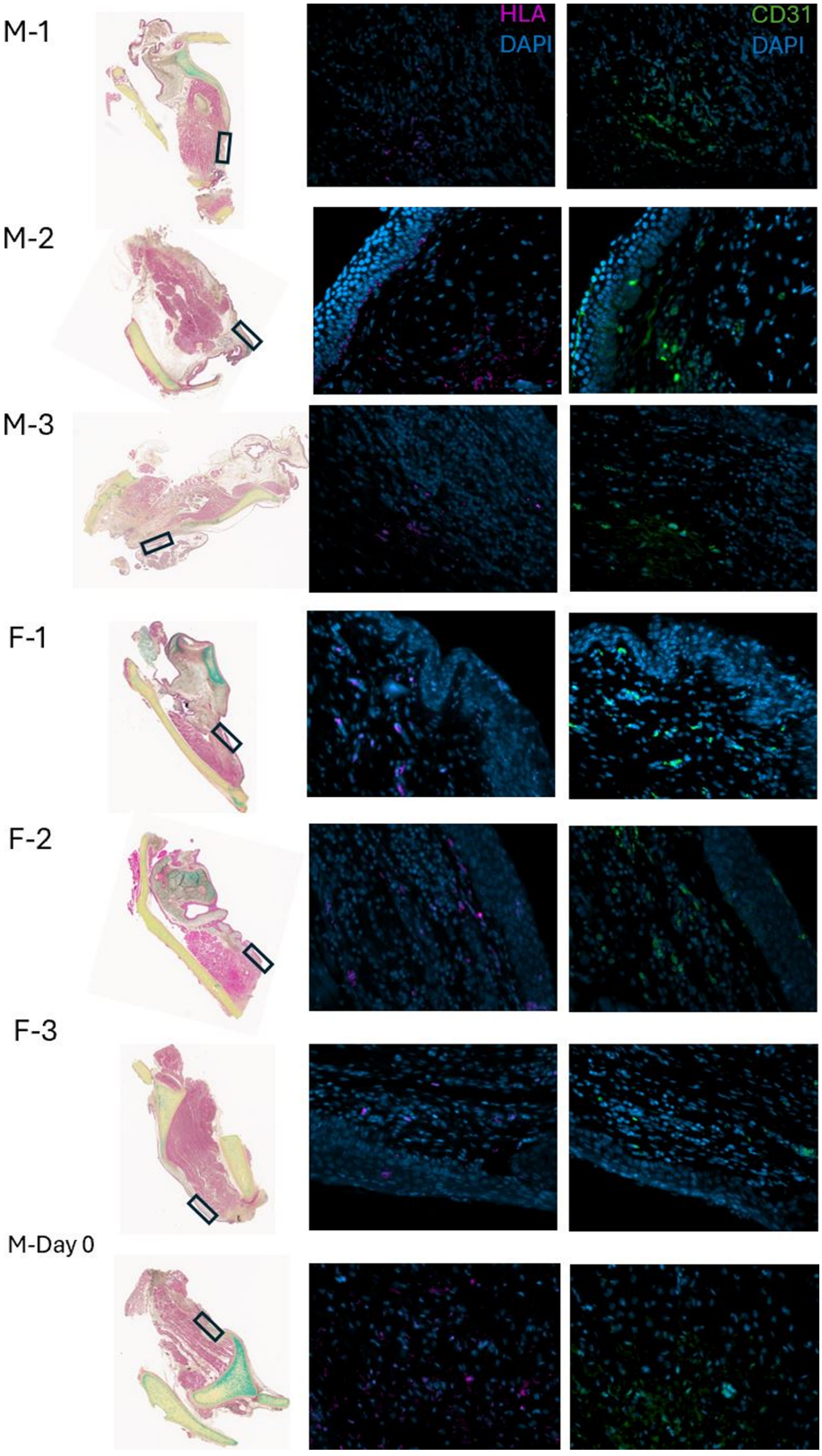

FIGURE 2 HLA and CD31 Labeling in COVR Implanted Tissue After Two Months. Microscopy from paraffin-embedded larynges. M and F denote male or female. Pentachrome stained sections at 4X show the full section of the vocal fold (VF), with the black box indicating the specific region of the slide from which images were taken. In the corresponding immunohistochemistry (IHC) images, HLA-positive cells are indicated with violet, and CD31-positive cells are marked with green. All images were taken at 40X magnification. The last row in the figure, M-Day 0, demonstrates more widespread HLA positivity in anthe animal that died immediately postoperatively.

(group 2, unilateral implant) were previously reported.[14] Scar group animals had no labeling for HLA, and BSA substitution for the HLA primary antibody eliminated labeling. Day 0 sections, from the animal suffering perioperative death, showed more HLA-positive cells than in the other animals. Still, cells in the implant region did not uniformly exhibit HLA, consistent with incomplete labeling due to antigen degradation or variable HLA expression by the cells.

3.2 | Vascular endothelial structure

CD31 was selected as a marker of vascular endothelium. It is also found in platelets and some types of leukocytes. Figure 2 demonstrates sections from the FFPE larynges, in which all animals underwent bilateral COVR implantation. All animals in this group demonstrated both HLA and CD31+ in the same area, anatomically corresponding to the implant site. The labeling quality was inadequate to identify if both markers were present in the same cells.

Figure 3 depicts the expression of CD31 and HLA, in frozen sections taken 2 months after COVR implantation or sham surgery.[14] CD31 expression was observed in all animals, whereas HLA-positive cells were only present in the Chronic COVR group.

In the Chronic COVR group, both CD31 and HLA-positive cells were present around lumenal structures that appear to be vascular endothelial in nature. In each of those animals, examples were found where HLA and CD31 appeared to be labeling the same cells in adjacent slides.

3.3 | Fibroblast activation state

Slides and tissues from a previously reported study[14] were probed here for SMA expression by immunocytochemistry and Western blot. Figure 4 shows IHC labeling for SMA and HLA in frozen sections 2 months after COVR implant or sham surgery. These markers were observed in nearby regions but did not appear to co-localize in individual cells in sequentially-cut sections. As anticipated, HLA was absent in all scar sections, consistent with the absence of implanted human cells. Figure 5 presents the quantification of SMA protein by Western blot in the chronic COVR, acute COVR, and scar groups. Expression levels varied in all groups, and there was no statistically significant difference in SMA expression among the three groups.

4 | DISCUSSION

Regenerative medicine, led by the use of stem cells, has provided an opportunity to develop treatments for tissue injury. Various cell lines from bone marrow, hematopoietic, epithelial, and adipose tissue have been derived. Compared to acellular or injection scaffolds, the COVR implant is unique in its structure as a bilayer of epithelial and mesenchymal cells within a fibrin matrix.

Our previous studies with COVR implantation in rabbit VFs found that human cells not only persisted in both acutely injured and chronically scarred VFs but that COVR also restored tissue microstructure and biomechanics.[13,14] Our work with COVR was also extended to a

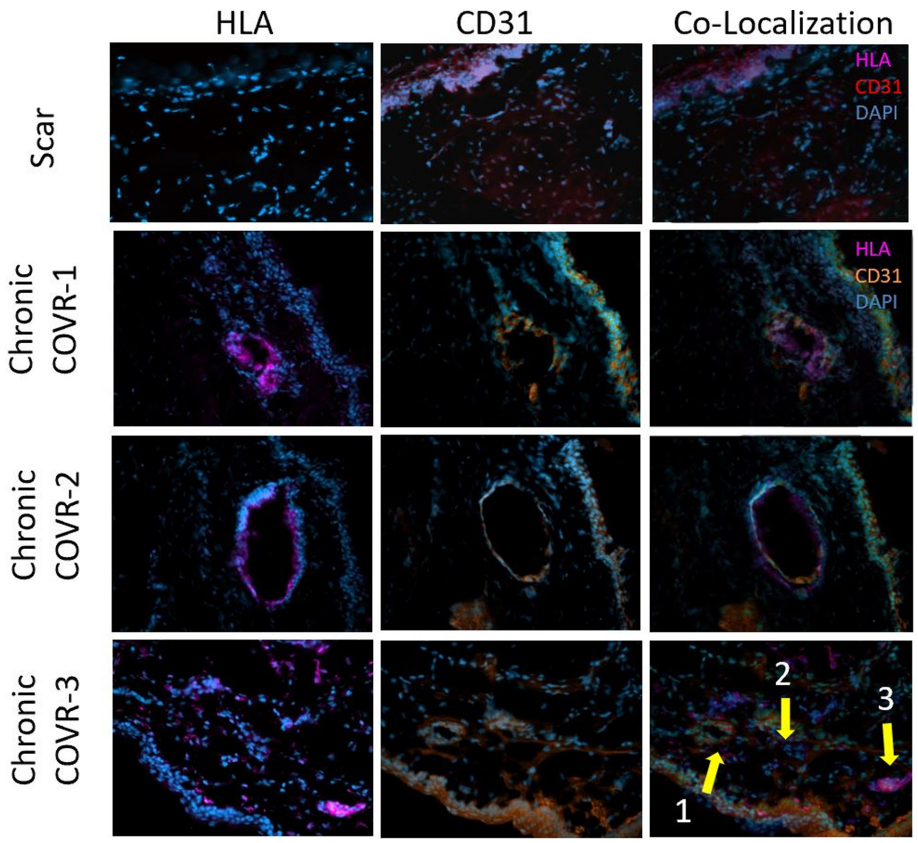

FIGURE 3 CD31 and HLA Expression in Chronic COVR vs Scar. All images were captured at 40X magnification. Each image in the Chronic COVR group represents a distinct animal. In the first row (Scar), HLA cells are stained violet, CD31 cells are stained red, and DAPI are stained blue. In the second, third, and fourth rows (Chronic COVR groups), HLA cells are stained violet, whereas CD31 cells are stained orange, and DAPI stained blue. The co-localization images were obtained by overlaying the respective HLA and CD31 images taken from sequentially cut slides. In the co-localization image for Chronic COVR-3, arrows 1 and 2 highlight a potential vascular structure where HLA-positive and CD31-positive cells overlap. Arrow 3 indicates a cluster of HLA-positive cells without co-localization of the CD31 marker.

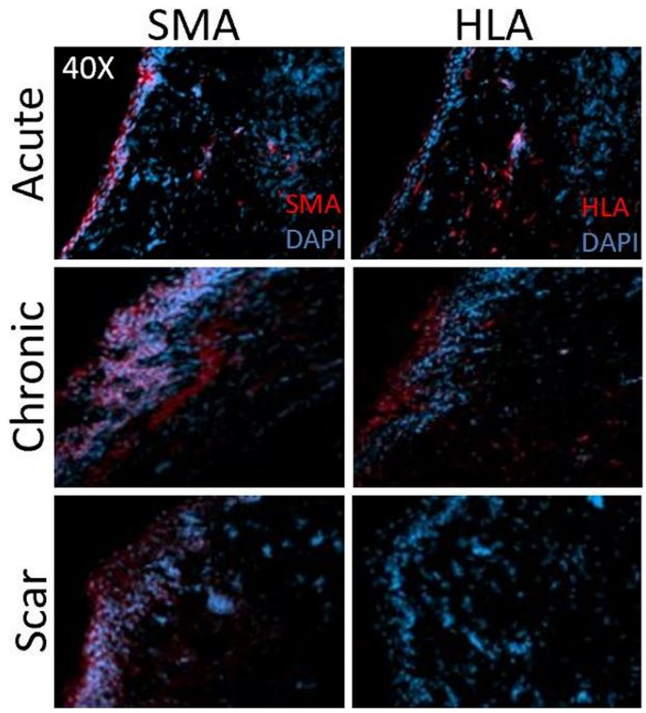

FIGURE 4 SMA and HLA labeling 2 months after surgery. Each treatment group is represented by a representative labeled section from one animal. Frozen sections were imaged at 40X magnification. All animals demonstrate positive staining for SMA. The presence of HLA is only observed in acute and chronic COVR groups with none visualized in scar. Co-localization of HLA and SMA within individual cells was not observed.

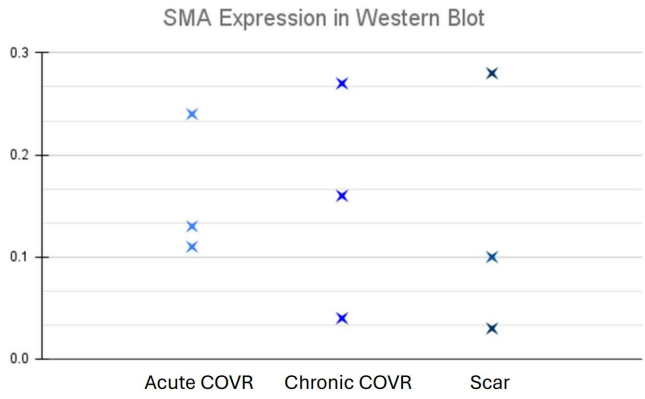

FIGURE 5 SMA Western blot quantification. Each "X" on the graph denotes one animal for which Western Blot was performed.; $n = 3$ in each of the three groups. *Y*-axis values are band intensity calculated via ImageJ analysis and normalized by a loading control band.

swine model, where preliminary studies demonstrated improved LP qualities, as well as improved acoustic parameters that reflected voice recovery.[19] Ongoing questions remain regarding mechanisms of functional improvement after COVR and ultimate cellular fates. This study further explores those questions.

4.1 | Vascular endothelial structure

The structure of human vocal folds is unique, as only small vessels are present near the vocal fold mucosa. This specific vascular structure, where small vessels are located at the vocal fold edge and separated from the vessels in other areas of the mucosa and muscle, helps to minimize hypoxia and ensures adequate vibration.[20] Assessing the vascular structure is therefore critical when evaluating the efficacy of vocal fold regeneration.

CD31, a common endothelial cell marker, plays an important role in vasculogenesis.[21] CD31+ endothelial progenitor cells have been identified within the stromal vascular fraction (SVF) of adipose tissue, from which hASCs are derived. Those cells were associated with the luminal layer of small blood vessels, and have the capacity to proliferate and form vessel-like structures.[22,23] SVF has separately been found to have the ability to differentiate into both endothelial and adipogenic cell types.[24]

To assess whether the COVR implant assisted with revascularization of the vocal folds, IHC labeling was performed for the endothelial marker CD31. In paraffin embedded sections, HLA and CD31 positive cells were visualized in similar areas. However, limited labeling in these FFPE sections made it difficult to determine if the markers co-localized. Frozen sections were then pursued because immunohistochemical labeling is typically more robust with this method.

These frozen sections more clearly exhibited co-localization of CD31 expression with hASC (as evidenced by HLA expression). This finding suggests that cells within the implanted COVR not only survive but also may develop donor-derived vascular structures. Scar group sections also demonstrated CD31 expression and vascular structures, without HLA, confirming that neovascularization occurs in the scar group during the normal wound healing process.

4.2 | Fibroblast activation state

Along the fibroblast–myofibroblast spectrum, myofibroblasts express α-SMA, and also produce excessive collagen, both leading to stiffening of the tissue.[25] The vocal fold fibroblast expression of α-SMA has been found to be decreased when the tissues were co-cultured with stem cells from either adipose or bone marrow sources.[25] Other previous work with mesenchymal stem cells has shown that their injection into scarred vocal folds can decrease the α-SMA expression and concurrently improve function.[26]

In the current study, we utilized α-SMA as a marker for myofibroblast activation. We hypothesized that COVR implantation would show a reduction in myofibroblast activation when compared to the scar group immunohistochemistry showed variable regions of SMA

expression within the implants and no co-localization with HLA. These findings suggest that the human ASC did not differentiate from myofibroblast phenotypes. However, there was no statistically significant difference in the bulk amount of SMA quantified among groups. We found no evidence, then, that hASC reduces myofibroblast phenotype among host cells in this system.

The variability observed could be due to intersubject differences within each treatment group. Potential sources of this variability could include different degrees of vocal fold injury as well as individual animal-to-animal variations. Further investigation is needed to fully elucidate the role of myofibroblasts and their activation state in the context of vocal fold scarring and the effects of the COVR implant.

5 | CONCLUSIONS

These results collectively provide insights into the cellular dynamics following COVR implantation after vocal fold resection in rabbits. Human ASC did not differentiate into a myofibroblast phenotype, although the COVR was not found to alter the overall SMA content within the tissue. Human ASC did co-localize with CD31 expression, suggesting that some implanted cells differentiated to a vascular endothelial phenotype. This finding requires further investigation to confirm. These findings continue to enrich our understanding of the complex interactions between implant and host tissue, offering valuable perspectives on the mechanisms of tissue repair and regeneration facilitated by COVR.

ACKNOWLEDGMENTS

We gratefully acknowledge the technical assistance of Carlos Castillo-Galdamez and the Division of Laboratory Animal Medicine.

FUNDING INFORMATION

This work was supported by the National Institutes of Health, NIDCD R01 DC016959 (J. Long). Additional support provided by: U.S. Department of Veteran Affairs, Rehabilitation Research and Development, I01RX003649; UCLA Jonsson Comprehensive Cancer Center; and NIH National Center for Advancing Translational Science (NCATS) UCLA CTSI Grant Number UL1TR001881.

CONFLICT OF INTEREST STATEMENT

The authors declare no conflicts of interest.

ORCID

Larissa Nicolas https://orcid.org/0009-0009-0886-6849
Jennifer L. Long https://orcid.org/0000-0002-4185-2328

REFERENCES

1. Hansen JK, Thibeault SL. Current understanding and review of the literature: vocal fold scarring. *J Voice*. 2006;20(1):110-120.
2. Kumai Y. Pathophysiology of fibrosis in the vocal fold: current research, future treatment strategies, and obstacles to restoring vocal fold pliability. *Int J Mol Sci*. 2019;20(10):2551.
3. Mattei A, Bertrand B, Jouve É, et al. Feasibility of first injection of autologous adipose tissue–derived stromal vascular fraction in human scarred vocal folds. *JAMA otolaryngol—Head Neck Surg*. 2020;146(4):355.
4. Ma Y, Long J, Amin MR, et al. Autologous fibroblasts for vocal scars and age-related atrophy: a randomized clinical trial. *Laryngoscope*. 2019;130(11):2650-2658.
5. Nagubothu SR, Sugars RV, Tudzarovski N, et al. Mesenchymal stromal cells modulate tissue repair responses within the injured vocal fold. *Laryngoscope*. 2019;130(1):E21-E29.
6. Li L, Stiadle JM, Lau HK, et al. Tissue engineering-based therapeutic strategies for vocal fold repair and regeneration. *Biomaterials*. 2016;108:91-110.
7. Fishman JM, Long J, Gugatschka M, et al. Stem cell approaches for vocal fold regeneration. *Laryngoscope*. 2016;126(8):1865-1870.
8. Cedervall J, Ährlund-Richter L, Svensson B, et al. Injection of embryonic stem cells into scarred rabbit vocal folds enhances healing and improves viscoelasticity: short-term results. *Laryngoscope*. 2007;117(11):2075-2081.
9. Svensson B, Srinivasa Nagubothu R, Cedervall J, et al. Injection of human mesenchymal stem cells improves healing of scarred vocal folds: analysis using a xenograft model. *Laryngoscope*. 2010;120(7):1370-1375.
10. Hiwatashi N, Hirano S, Mizuta M, et al. Adipose-derived stem cells versus bone marrow-derived stem cells for vocal fold regeneration. *Laryngoscope*. 2014;124(12):E461-E469.
11. Hong SJ, Lee SH, Jin SM, et al. Vocal fold wound healing after injection of human adipose-derived stem cells in a rabbit model. *Acta Otolaryngol*. 2011;131(11):1198-1204.
12. Tchoukalova YD, Zacharias SRC, Mitchell N, et al. Human amniotic epithelial cell transplantation improves scar remodeling in a rabbit model of acute vocal fold injury: a pilot study. *Stem Cell Res Ther*. 2022;13(1):31.
13. Tran EK, Alhiyari Y, Juarez K, et al. A xenograft study of human adipose stromal cell-based vocal fold mucosal replacement in rabbits. *Laryngoscope Investig Otolaryngol*. 2022;7(5):1521-1531.
14. Rodell S, Schlegel P, Zhang Z, Reddy N, Yazeed A, Long JL. Cell-based outer vocal fold replacement both treats and prevents vocal fold scarring in rabbits. *Laryngoscope*. 2024;134(2):764-772.
15. Goel AN, Gowda BS, Veena MS, Shiba TL, Long JL. Adipose-derived mesenchymal stromal cells persist in tissue-engineered vocal fold replacement in rabbits. *Ann Otol Rhinol Laryngol*. 2018;127(12):962-968.
16. Long JL, Zuk P, Berke GS, Chhetri DK. Epithelial differentiation of adipose-derived stem cells for laryngeal tissue engineering. *Laryngoscope*. 2009;120(1):125-131.
17. ImageJ. Gels Submenu. Accessed January 2024. https://imagej.net/ij/docs/menus/analyze.html#gels
18. Stael S, Miller LP, Fernández-Fernández ÁD, Van Breusegem F. Detection of damage-activated metacaspase activity by Western Blot in plants. In: Klemencic M, Stael S, Huesgen PF, eds. *Plant Proteases and Plant Cell Death: Methods and Protocols*. Springer US; 2022:127-137.
19. Schlegel P, Yan K, Upadhyaya S, et al. Tissue-engineered vocal fold replacement in swine: methods for functional and structural analysis. *PLoS One*. 2023;18(4):e0284135.
20. Sato K. *Functional Histoanatomy of the Human Larynx*. Springer Nature Singapore; 2018.
21. Duncan G, Andrew DP, Takimoto H, et al. Genetic evidence for functional redundancy of platelet/endothelial cell adhesion Molecule-1 (PECAM-1): CD31-deficient mice reveal PECAM-1-dependent and PECAM-1-independent functions. *J Immunol*. 1999;162(5):3022-3030.
22. Zimmerlin L, Donnenberg VS, Pfeifer ME, et al. Stromal vascular progenitors in adult human adipose tissue. *Cytometry A*. 2010;77(1):22-30.
23. Zimmerlin L, Donnenberg VS, Rubin JP, Donnenberg AD. Mesenchymal markers on human adipose stem/progenitor cells. *Cytometry A*. 2012;83A(1):134-140.

24. Wosnitza M, Hemmrich K, Groger A, Gräber S, Pallua N. Plasticity of human adipose stem cells to perform adipogenic and endothelial differentiation. *Differentiation*. 2007;75(1):12-23.
25. Hiwatashi N, Bing R, Kraja I, Branski RC. Mesenchymal stem cells have antifibrotic effects on transforming growth factor-β1-stimulated vocal fold fibroblasts. *Laryngoscope*. 2016;127(1):E35-E41.
26. Mattei A, Magalon J, Bertrand B, Philandrianos C, Veran J, Giovanni A. Cell therapy and vocal fold scarring. *Eur Ann Otorhinolaryngol Head Neck Dis*. 2017;134(5):339-345.

How to cite this article: Nicolas L, Mandl H, Schrader F, Long JL. Immunocytochemistry assessment of vocal fold regeneration after cell-based implant in rabbits. *Laryngoscope Investigative Otolaryngology*. 2024;9(5):e70007. doi:10.1002/lio2.70007